*J. Fluid Mech.* (1972), *vol.* 55, *part* 1, *pp.* 149–161
*Printed in Great Britain*



# Transmission of water waves through small apertures

By D. C. GUINEY, B. J. NOYE AND E. O. TUCK
Department of Applied Mathematics, University of Adelaide

(Received 27 March 1972)

The water-wave transmission coefficient for a small slit in a thick vertical barrier is obtained theoretically and verified both experimentally and by comparison with an exact theory for the case of zero thickness. Similar shallow-water results are presented.

## 1. Introduction

The theory of Tuck (1971, hereafter denoted by I) concerns water-wave transmission through small horizontal slits in a vertical barrier of zero thickness. The fluid is supposed infinitely deep and the barrier is impermeable over its whole infinite height apart from the single slit. The resulting formula for the transmission coefficient predicts that a remarkably high proportion of the incident energy is transmitted through quite small slits.

The present paper is a continuation of the work of I, with the objective of verifying the accuracy of I both theoretically and experimentally, and of extending the theory to account for finite barrier thickness and shallow-water effects. Theoretical confirmation of the approximate theory in I is provided by use of recent exact results of Guiney (1972) and Porter (1972) based on the general theories of Lewin (1963) and Mei (1966). Comparison of exact and approximate results for zero thickness suggests that the small-gap approximation remains accurate even up to gap sizes comparable with the mean submergence of the slit.

Experimental confirmation of the theory of I was attempted by a specially designed set of experiments. However, the measured transmitted energy was low (typically 70 %) relative to the predictions of I. Although it was suspected that dissipation might be the cause of this discrepancy, the problem of accounting for non-zero barrier thickness was also considered.

The extension of the theory of I to incorporate a barrier thickness of the same order of magnitude as the (small) gap size is quite straightforward, the formula for the transmission coefficient now involving certain elliptic integrals which arise from the conformal mapping of the rectangular gap geometry. The predicted effect of the wall thickness is a substantial decrease in transmission, and indeed the new theory agrees very well with the experimental results, suggesting that dissipation is not in fact significant in the present problem.

Finally a simple theoretical treatment of the corresponding shallow-water problem is given. Shallow water in this context means *very* shallow water, such that the incident wavelength is much greater than the water depth. The resulting

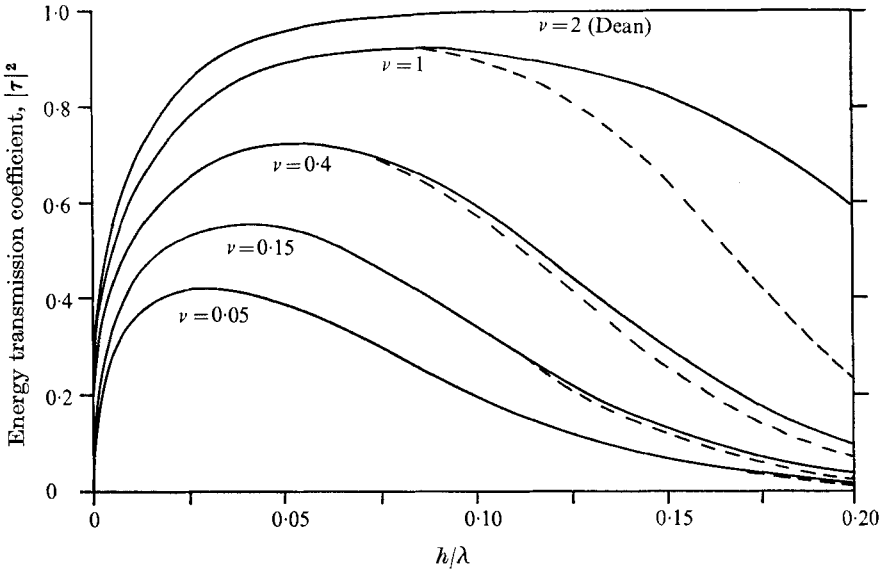


FIGURE 1. Comparison between exact transmission computations (Guiney 1972, solid line) and small-gap theory (Tuck 1971, broken line) for zero wall thickness.

transmission coefficient is characterized by a single parameter, the blockage coefficient of the aperture. This blockage coefficient is independent of wave properties, depending only on the geometric shape of the aperture, and may be calculated easily for a number of given geometries. Similar problems have been discussed by Ogilvie (1969).

## 2. Comparison of exact and approximate results for zero-thickness barriers

An 'exact solution' for the problem of plane water waves incident on a zero-thickness vertical barrier containing any number of horizontal slits of any width was given by Lewin (1963) and Mei (1966). These theories did not, however, enable direct specialization to provide the transmission coefficient for a single slit, and Porter (1972) and Guiney (1972) used somewhat different methods to solve this special problem. Even for this simple problem the solution for the transmission coefficient involves a very complicated numerical integration and we refer to the original papers for the details. Our purpose here is merely to present some computed results of Guiney (1972) which provide a comparison with the small-gap theory of I.

Figure 1 shows the energy transmission coefficient $|\tau|^2$ as a function of wavelength, plotted non-dimensionally as $h/\lambda$, where $h$ is the depth of submergence of the slit. The parameter $\nu$ is defined as

$$\nu = 2a/h, \tag{2.1}$$

where $2a$ is the width of the slit. The dashed curves (apart from the $\nu = 1$ curve)

were presented in I and are computed from the small-gap approximation (i.e. for small $\nu$), whereas the solid curves are obtained by numerical integration using the exact formulae of Guiney (1972), valid for arbitrary $\nu$.

When $\nu = 0{\cdot}05$, which describes a very small gap, the results agree to three significant figures in the range of the graph. At higher values of $\nu$ the small-gap theory is accurate to about two figures at frequencies below the maximum of transmission and only begins to become inaccurate in the high frequency tails of the curves. It is remarkable that even for $\nu = 1$, when the width of the slit is twice the depth of its upper edge, so that we can hardly call the gap small, the small-gap theory is still useful up to and including the point of maximum transmission.

The curve for $\nu = 2$ shown corresponds to the case of a submerged barrier, the top edge of the gap having moved above the free surface. This problem was solved by Dean (1945), and the present results agree accurately with those of Dean. Guiney (1972) has also verified Ursell's (1947) results for a vertical surface-intersecting barrier of finite depth, in the limit as the lower edge of the slit goes to $-\infty$.

## 3. Effect of wall thickness

In this section we extend the theory of I to account for non-zero barrier thickness. We retain the small-gap approximation and the inner and outer flow picture as in I. In the outer region, far from the slit, the flow is source-like on one side and sink-like on the other side of the barrier, the free surface having a significant effect. On the other hand, in the inner region near the slit the free surface is assumed to have no effect, and the flow through the slit is obtained by conformal mapping.

For the zero-thickness barrier in I, a Joukowski mapping was sufficient to solve the inner problem, but for more general geometries essentially the same solution procedure applies, so long as a conformal mapping function which transforms the region bounded by the aperture contour into an upper half complex plane is known. Once this mapping has been carried out, we can easily match the source-like behaviour at 'infinity' for the inner solution with the appropriate outer source solution.

The specific flow situation of interest is shown in figure 2. The barrier has breadth $2b$ and a gap of size $2a$ is situated at mean submergence $h$ below the free surface in an infinite depth of water. We define the parameter $\nu$ as in (2.1) and define

$$\gamma = b/a \tag{3.1}$$

and assume $\nu$ to be small, while $\gamma = O(1)$. We must solve for a velocity potential $\phi(x, y, t)$ satisfying Laplace's equation for $y < 0$ and the linearized free-surface condition (see I) on $y = 0$.

The far-field conditions are as in I, namely

$$\phi \to \mathscr{R}[A_I e^{-i\kappa z + i\sigma t} + \rho A_I e^{+i\kappa z + i\sigma t}] \tag{3.2}$$

as $x \to -\infty$, and

$$\phi \to \mathscr{R}[\tau A_I e^{-i\kappa z + i\sigma t}] \tag{3.3}$$

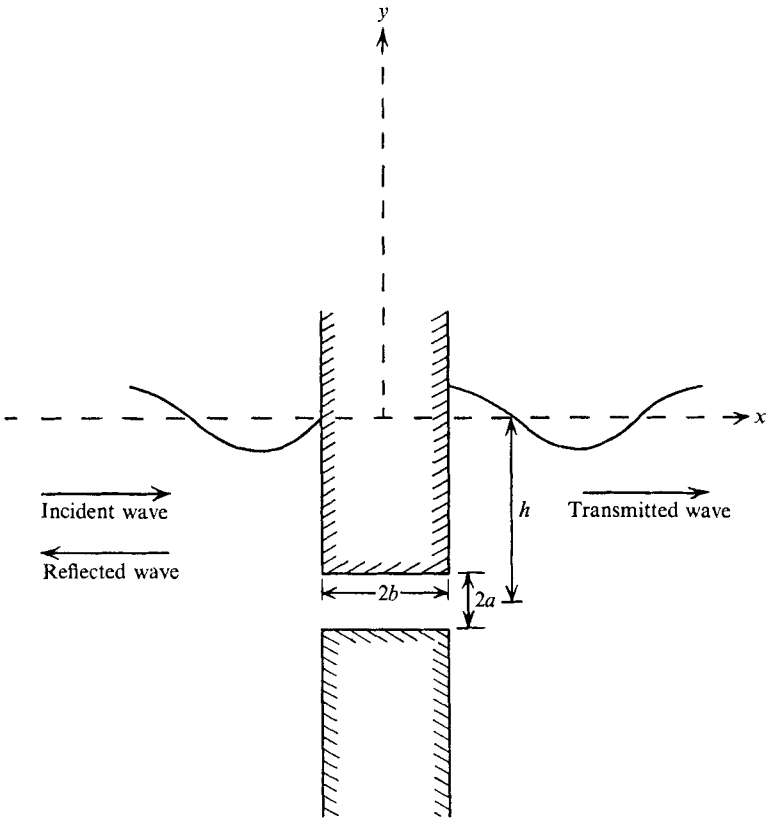


FIGURE 2. Sketch of geometry of thick barrier.

as $x \to +\infty$, $\kappa = \sigma^2/g$ being the wavenumber, $A_I$ the (arbitrary) incident wave amplitude and $z = x + iy$. The quantities $\rho$ and $\tau$ are complex reflexion and transmission coefficients, to be determined.

Since we are taking $\gamma = O(1)$, far from the gap at distances of $O(h)$ both gap size and barrier thickness tend to zero as $\nu \to 0$. Thus the outer problem is *identical* to that for the zero-thickness barrier and the solution of I applies. We merely need to extract the information that as we approach the gap we have

$$\phi \to \pm \frac{\cos \sigma t}{2\pi} \log (z + ih) + C_{\pm}, \tag{3.4}$$

as $z \to 0_{\pm} + ih$, where

$$C_+ = \left[ -\frac{1}{2\pi} \log (-2ih) - \frac{1}{\pi} \int_0^{\infty} \frac{e^{-2kh}}{k - \kappa} dk \right] \cos \sigma t - e^{-2\kappa h} \sin \sigma t \tag{3.5}$$

and

$$C_- = -C_+ + e^{-2\kappa h} (A \cos \sigma t + B \sin \sigma t), \tag{3.6}$$

$A$ and $B$ being real constants to be determined, such that

$$\tau = 2i/(A - iB). \tag{3.7}$$

In the inner region we suppose that the free surface is too far away to have any effect, and hence must solve the problem of streaming flow through a finite

rectangular aperture in a wall of thickness $2b$ in an infinite fluid, the flow being source–sink-like at infinity. The required mapping is of the Schwartz–Christoffel type (Davy 1944) and is defined by

$$\frac{dz}{d\zeta} = \frac{i\alpha[(k^2\zeta^2-1)(\zeta^2-1)]^{\frac{1}{2}}}{\zeta^2}, \tag{3.8}$$

with branch cuts along the line segments

$$1 < |\mathscr{R}\zeta| < k^{-1}. \tag{3.9}$$

Here $k$ is the positive root of

$$\gamma = \frac{K'k'^2 - 2K' + 2E'}{2(Kk'^2 - 2E)} \tag{3.10}$$

and

$$-\alpha = a/(2E - k'^2K), \tag{3.11}$$

with

$$k'^2 = 1-k^2, \quad K' = K(k'), \quad \text{etc.} \tag{3.12}$$

The functions $K(k)$ and $E(k)$ are complete elliptic integrals of the first and second kind respectively (Abramowitz & Stegun 1964, p. 590).

The solution for a source of strength $m$ at the origin in the $\zeta$ plane is

$$\phi = \mathscr{R}[(m/2\pi)\log\zeta + C] \tag{3.13}$$

for some constant $C$. Now as $\zeta \to 0$ we are looking at the flow in the neighbourhood of the point $D$ in both $z$ and $\zeta$ planes (figure 3). In the $z$ plane this corresponds to an infinite semicircle on the left-hand side, and hence $x \to -\infty$. Thus from (3.8)

$$dz/d\zeta \to -i\alpha/\zeta^2, \tag{3.14}$$

so that

$$z + ih \to i\alpha/\zeta$$

and hence as $x \to -\infty$

$$\phi \to \mathscr{R}\left[-\frac{m}{2\pi}\log(z+ih) + C + \frac{m}{2\pi}\log i\alpha\right]. \tag{3.15}$$

Similarly, as $\zeta \to \infty$, we have $x \to +\infty$, and

$$dz/d\zeta \to i\alpha k,$$

which implies that

$$z + ih \to i\alpha k\zeta$$

and therefore

$$\phi \to \mathscr{R}\left[\frac{m}{2\pi}\log(z+ih) + C - \frac{m}{2\pi}\log i\alpha k\right]. \tag{3.16}$$

Matching the near-field behaviour (3.4) of the outer solution with the far-field behaviour (3.15) and (3.16) of the inner solution gives

$$m = \cos\sigma t, \quad C_+ = C - \frac{\cos\sigma t}{2\pi}\log i\alpha k \tag{3.17}$$

and

$$C_- = C + \frac{\cos\sigma t}{2\pi}\log i\alpha. \tag{3.18}$$

Thus

$$C_+ - C_- = \frac{\cos\sigma t}{2\pi}\log(-\alpha^2 k). \tag{3.19}$$

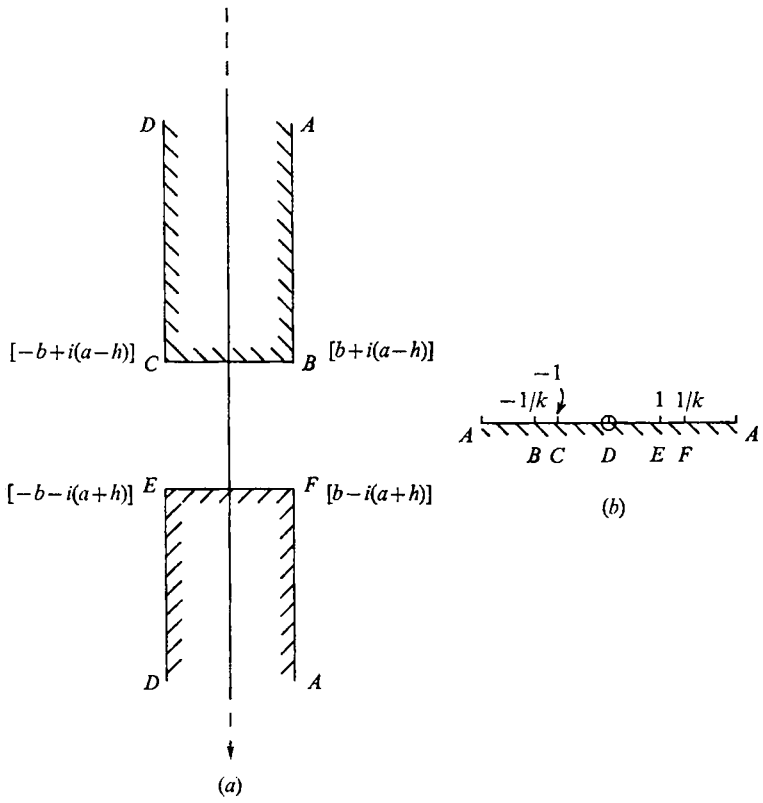


FIGURE 3. Conformal mapping of the inner region. (a) $z$ plane, (b) $\zeta$ plane.

When (3.6) has been solved for $C_+$, (3.19) gives

$$2C_+ = e^{-2\kappa h}(A\cos\sigma t + B\sin\sigma t) - \frac{\cos\sigma t}{2\pi}\log(-\alpha^2 k), \tag{3.20}$$

from which $A$ and $B$ follow by equating coefficients of $\cos\sigma t$ and of $\sin\sigma t$ in (3.5). Thus

$$B = -2 \tag{3.21}$$

and

$$A = \frac{1}{\pi}\log\left(-\frac{\alpha k^{\frac{1}{2}}}{2h}\right)e^{2\kappa h} + \frac{2}{\pi}\bar{E}i(2\kappa h), \tag{3.22}$$

$\bar{E}i$ being an exponential integral. Finally, the transmission coefficient $\tau$ follows from (3.7), and we have

$$|\tau|^{-2} = 1 + \left[\frac{1}{2\pi}e^{2\kappa h}\log\left(-\frac{\alpha k^{\frac{1}{2}}}{2h}\right) + \frac{1}{\pi}\bar{E}i(2\kappa h)\right]^2. \tag{3.23}$$

Considering now the limiting case when the width of the barrier tends to zero, i.e. $\gamma \to 0$, it is clear geometrically and by the properties of the elliptic functions that $k \to 1$, and thus (3.11) gives

$$-\alpha \to \tfrac{1}{2}a, \tag{3.24}$$

so that

$$|\tau|^{-2} \to 1 + \left[\frac{1}{2\pi}e^{2\kappa h}\log\frac{a}{4h} + \frac{1}{\pi}\bar{E}i(2\kappa h)\right]^2, \tag{3.25}$$

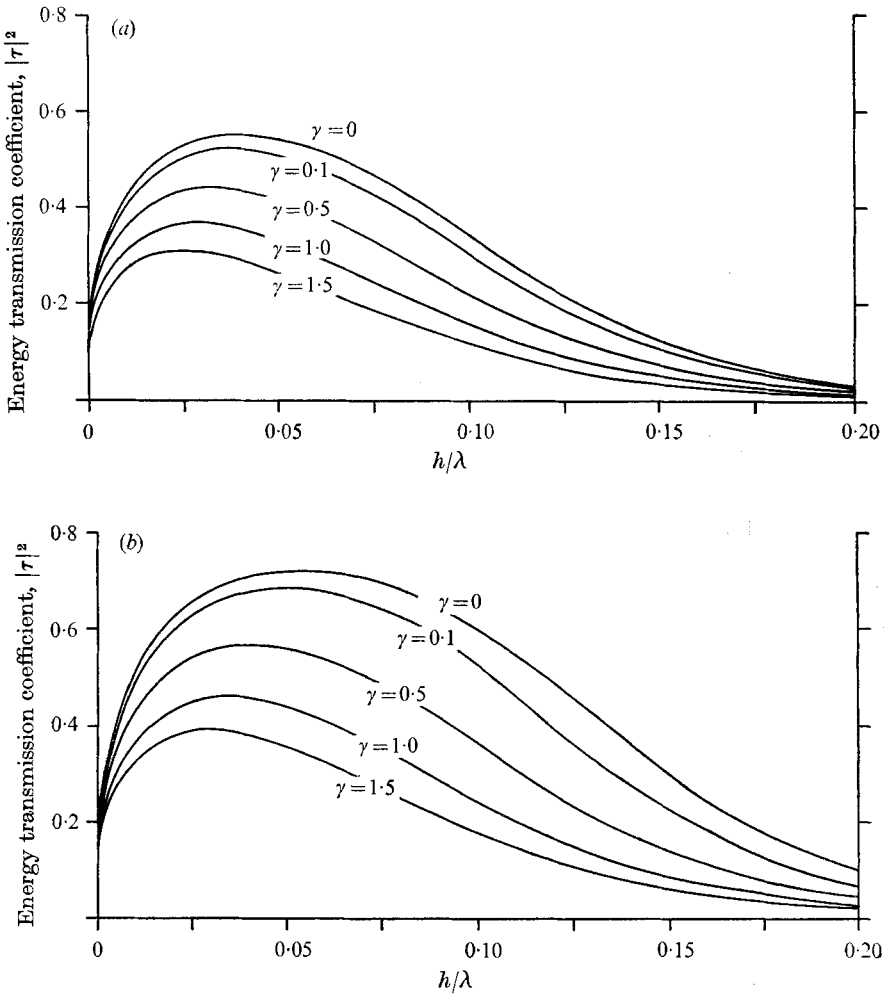


FIGURE 4. Effect of wall thickness at (*a*) $\nu = 0{\cdot}15$, and (*b*) $\nu = 0{\cdot}40$.

which is the solution found in I. Note that the expressions (3.23) and (3.25) differ only in the argument of the logarithmic term.

Figures 4 (*a*) and (*b*) show computed curves of $|\tau|^2$ *vs.* $h/\lambda = (1/2\pi)\,\kappa h$ for various values of $\nu$ and $\gamma$. Non-zero barrier thickness always reduces transmission relative to the zero-thickness results, at fixed $\nu$ and $h/\lambda$. At very low frequencies the exponential integral term in (3.23) dominates and the thickness $\gamma$ has little effect. However, at and above the frequency of maximum energy transmission the effect of $\gamma$ is very pronounced, and the thickness substantially reduces maximum transmission. The frequency at which maximum transmission occurs also tends to be a little lower for thick barriers.

A solution can also be obtained (Guiney 1972) in the case when $\gamma$ is large, for example when the barrier thickness is as much as the gap submergence: $2b = O(h) \gg O(2a)$. It turns out, however, that the result (3.23) above is uniformly

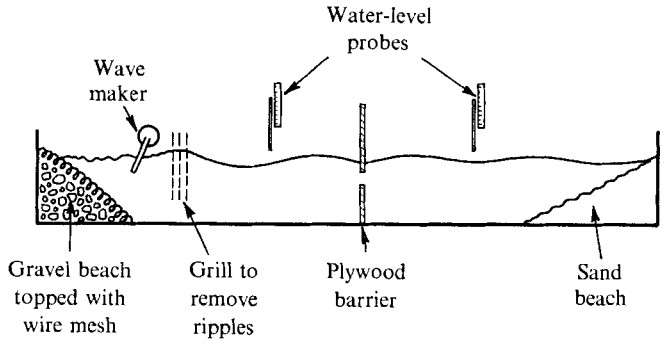


FIGURE 5. Sketch of experimental set-up.

valid in that it gives the correct limit as $\gamma \to \infty$ as well as for $\gamma \to 0$, namely as $\gamma \to \infty$

$$|\tau|^{-2} = 1 + \left[\frac{1}{2\pi} e^{2\kappa h}\left(\log\frac{2a}{h} - 1 - \frac{\pi}{2}\gamma\right) + \frac{1}{\pi}\bar{E}i(2\kappa h)\right]^2, \tag{3.26}$$

which corresponds to $k \to 0$ in (3.11). Note that (3.26) implies in the limit $\gamma \to \infty$ that at fixed $\nu$ and $h/\lambda$ there is no transmission through an infinitely wide barrier, as is expected physically.

Although the results of the present section are only for small gaps (i.e. small $\nu$), the good agreement shown in the previous section between the small-gap theory at zero thickness and the exact (i.e. finite $\nu$) theory gives reason to expect that $\nu$ need not be too small in order that the finite-thickness result (3.23) be useful.

## 4. Experimental results

A series of experiments was carried out in water of depth 70 cm in a flume of rectangular cross-section and of length 33 m and width 1·3 m, in the Department of Civil Engineering, University of Adelaide. A paddle-type wave maker was located near one end, and a vertical barrier of 0·80 cm thick marine plywood was fitted about 12 m from the wave maker, dividing the flume into two nearly equal parts. The barrier was arranged so that horizontal slits of width either 2·54 cm or 3·80 cm extending across the full width of the flume could be set with their centre-lines at depths of 10·2 cm, 15·2 cm or 22·9 cm below the mean water level. The experimental configuration is shown diagrammatically in figure 5.

Incident and transmitted wave amplitudes were measured in the following manner using water-level probes potentially accurate to 0·02 cm. The mean water level was noted on each probe when the wave maker was adjusted to produce waves of a suitable known frequency. The wave maker was then switched off and all motion allowed to cease before actual measurements were commenced.

When the wave maker was switched on again, one observer quickly adjusted by eye the water-level probe on the incident side of the barrier so that its tip barely touched the top of the passing wave crests. This had to be done after the initial transient stage so that pure sinusoidal incident waves were fully developed, but before the reflected waves from the barrier began to affect the wave pattern

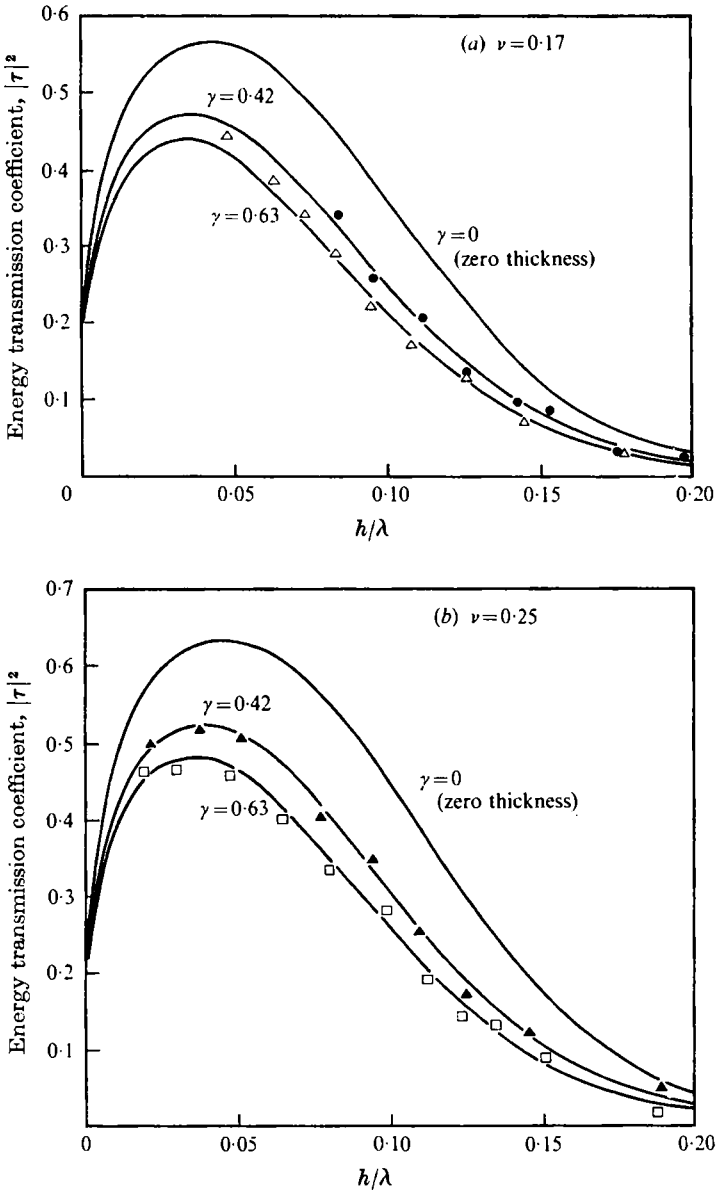


FIGURE 6. Comparison of theoretical (solid lines) and experimental results. (*a*) $\nu = 0{\cdot}17$: ●, $\gamma = 0{\cdot}42$; △, $\gamma = 0{\cdot}63$. (*b*) $\nu = 0{\cdot}25$: ▲, $\gamma = 0{\cdot}42$; □, $\gamma = 0{\cdot}63$.

between it and the wave maker. On the other side of the barrier, a second observer carried out the same procedure to measure the transmitted wave amplitude.

The wave maker was then switched off, the water in the flume allowed to come to rest and the process repeated. This time, of course, the probes were already set near the top of the wave crests, so a more accurate setting could be made, using a vernier scale. After several such runs the instrument settings were finally checked by connecting the metal probes to a d.c. power supply with a lamp in

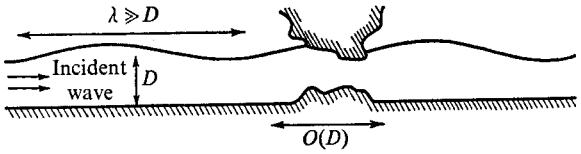


FIGURE 7. Sketch of shallow-water transmission problem.

series; a correctly set probe produced a very brief flash of light as it made only momentary contact with the top of the wave. Although time consuming, the whole process was repeated up to six times per frequency, until successive readings were sensibly identical.

From the amplitude readings obtained, the energy transmission coefficient was calculated, and these results are plotted in figures 6 (*a*) and (*b*). A qualitative conclusion immediately evident, and in agreement with the results of the previous section, is that larger values of $\gamma$ (= barrier thickness/slit width) produce lower transmission coefficients, at the same values of $h/\lambda$ and $\nu$ (= slit width/slit submergence).

These experiments were actually carried out at a time when only the theoretical results of I for the infinitesimally thick barrier ($\gamma = 0$) were available, and the experimental results appeared to be disappointingly low relative to the theory of I. The assumed reason for this discrepancy was energy dissipation of various kinds. Indeed, in some cases jet-like or eddying behaviour was noted in the flow through the slit. However, when the theoretical results for the finite barrier thickness became available it was soon clear that these apparent anomalies in the experimental results were amply explained by taking into account barrier thickness. In fact the agreement in figure 6 is sufficiently close to suggest that dissipative effects did not significantly affect wave transmission through finite-width slits, even in those cases where observation suggested they were present to some extent in the local flow through the slit.

Because the water depth could not exceed 70 cm, the first two or three experimental points to the left of each graph correspond to wavelengths which perhaps exceed the usual criteria for applicability of deep-water theory (e.g. 'depth greater than about half a wavelength'). However, the effect on the results appears to be quite small. No experiments were performed in truly shallow-water conditions (wavelength much greater than water depth), such as those assumed in the following section.

## 5. Shallow-water theory

The effects of the bottom on the experimental results of the previous section come under the heading of 'finite-depth' effects, since they correspond to situations where the wavelength and water depth are comparable. A finite-depth extension of I is possible, but tedious and numerically complicated, whereas a shallow-water theory valid at the other extreme from I when the wavelength $\lambda$ is much greater than the depth $D$ is quite straightforward to construct.

Indeed we can quite easily solve formally for transmission of shallow-water

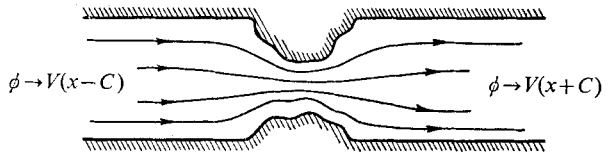


FIGURE 8. Inner problem for shallow-water case, arbitrary geometry of aperture.

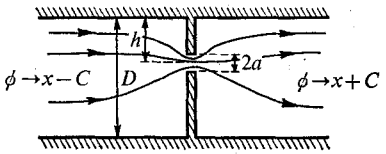


FIGURE 9. Inner problem for special case of small gap in wall of zero thickness in shallow water.

waves through an aperture or past an obstruction of arbitrary shape and size (figure 7) as follows. If $\lambda \gg D$, shallow-water theory (Wehausen & Laitone 1960) requires the velocity potential $\phi$ to satisfy the one-dimensional wave equation

$$\phi_{tt} = gD\phi_{xx} \tag{5.1}$$

in an outer region $|x| \gg D$ which excludes only the immediate neighbourhood of the disturbance. The only acceptable solution possessing sinusoidal time dependence is thus the real part of

$$\phi = \begin{cases} e^{-ikx+i\sigma t} + \rho\, e^{+ikx+i\sigma t} & (x \ll -D), \\ \tau\, e^{-ikx-i\sigma t} & (x \gg D), \end{cases} \tag{5.2}$$

where $\sigma = (gD)^{\frac{1}{2}} k$ and $\rho$ and $\tau$ are the reflexion and transmission coefficients, as in (3.3) and (3.4) with $A_I$ taken as unity without loss of generality.

The inner expansion of the outer solution (5.2) is ($|x|/D \to 0$)

$$\phi = \begin{cases} (1+\rho)\, e^{i\sigma t} - ik(1-\rho)\, e^{i\sigma t}\, x, \\ \tau\, e^{i\sigma t} - ik\tau\, e^{i\sigma t}\, x. \end{cases} \tag{5.3}$$

This must match an inner solution valid for $x = O(D)$, in which the free surface may be replaced by a rigid wall to leading order. This flow is shown in figure 8 and represents streaming at velocity $V$ through the aperture, there being a jump $2CV$ in the disturbance potential $\phi - Vx$ between $x = -\infty$ and $x = +\infty$.

The problem sketched in figure 8 may be solved numerically without difficulty for an arbitrary aperture geometry (Tuck & Taylor 1970; Taylor 1971). The constant $C$ is a unique property of the aperture geometry, described by Tuck & Taylor (1970) as a 'blockage' coefficient† and computed for some similar problems by Newman (1969), Flagg & Newman (1971) and Taylor (1971). As an example,

† $C$ can also be related in an electrostatic analogy to the change in capacitance of a parallel-plate condenser, due to a deformation of the plates such that they follow the contours of the obstruction.

we give in the appendix an approximate evaluation of $C$ for a small slit of width $2a \ll D$ at a depth $h$ in an infinitesimally wide wall (figure 9). The result is

$$C = -\frac{D}{\pi}\log\left(\pi\frac{a}{D}\sin\frac{\pi h}{D}\right). \tag{5.4}$$

Now on matching fluxes through the aperture we obtain from (5.3)

$$V = -ik(1-\rho)\,e^{i\sigma t} = -ik\tau\,e^{i\sigma t} \tag{5.5}$$

and on matching the jump in potential we obtain

$$2CV = \tau\,e^{i\sigma t} - (1+\rho)\,e^{i\sigma t}. \tag{5.6}$$

Thus
$$\rho + \tau = 1 \tag{5.7}$$

and
$$-2Cik\tau = \tau - 1 - \rho. \tag{5.8}$$

Hence
$$\tau = 1/(1+ikC) \tag{5.9}$$

and
$$|\tau|^2 = 1/(1+k^2C^2). \tag{5.10}$$

The result (5.10) is remarkably simple, and indicates the direct effect of the blockage coefficient $C$ on the transmission. All curves of $|\tau|^2$ against $k$ are similar in shape irrespective of the aperture geometry, decreasing from unity (perfect transmission) at zero frequency to zero at infinite frequency, the decay rate being such that half of the incident energy is reflected at $k = 1/C$. Since $C$ is in most cases numerically large compared with the depth $D$ (as is indicated by (5.4) for $a/D$ or $h/D$ small), transmission only occurs for wavelengths significantly greater than water depth $D$, confining attention to the strictly shallow-water range.

## Appendix

To solve the problem illustrated by figure 9 (in which we have set $V = 1$) we make use of a Green's function for the channel $-D < y < 0$ (Taylor 1971), i.e.

$$\Phi = \frac{D}{\pi}\mathscr{R}\left\{\log\left[4\sinh\left(\frac{\pi}{2D}(z+ih)\right)\sinh\left(\frac{\pi}{2D}(z-ih)\right)\right]\right\}, \tag{A 1}$$

where $z = x+iy$. This function represents a source of strength $2D$ located at $(0, -h)$, satisfying $\Phi_y = 0$ on $y = 0, -D$. It has the following properties:

$$\Phi \to \pm x \quad \text{as} \quad x \to \pm\infty, \tag{A 2}$$

$$\Phi \to (D/\pi)(\log r + K) \quad \text{as} \quad r \to 0, \tag{A 3}$$

where
$$K = \log\frac{2\pi}{D}\sin\frac{\pi h}{D}. \tag{A 4}$$

If $2a \ll D$, the aperture in figure 5.3 can be represented by a source for $x > 0$ and a sink for $x < 0$, i.e.

$$\phi = \pm(\Phi + C). \tag{A 5}$$

In view of (A 2), this solution satisfies the correct boundary condition as $x \to \pm\infty$; our task is to determine $C$.

The solution near the aperture is that for streaming flow through a gap in an *infinite* wall, which can be obtained (see I) by a Joukowski mapping. Matching with (A 5), using (A 3), gives

$$\phi \to \pm \frac{D}{\pi}\left(\log r + K + \frac{\pi C}{D}\right) \quad \text{as} \quad \frac{x}{2a} \to \pm\infty. \tag{A 6}$$

However, a property of the aperture flow (I) is that if $\phi \to \pm V(\log r + C_1)$ as $x \to \pm\infty$, then $C_1 = -\log \frac{1}{2}a$. Thus

$$K + \pi C/D = -\log \tfrac{1}{2}a \tag{A 7}$$

and, using (A 4),

$$C = -\frac{D}{\pi}\log\frac{\pi a}{D}\sin\frac{\pi h}{D}. \tag{A 8}$$

The special case $h = \frac{1}{2}D$ gives least blockage, i.e.

$$C = -\frac{D}{\pi}\log\frac{\pi a}{D}. \tag{A 9}$$

This last result (A 9) is the limit as $a/D$ tends to zero of an exact result of Sedov (see Newman 1969) for arbitrary $a/D$, namely

$$C = -\frac{D}{\pi}\log\sin\frac{\pi a}{D}. \tag{A 10}$$

## REFERENCES


Abramowitz, M. & Stegun, L. A. (eds.) 1964 *Handbook of Mathematical Functions.* Washington: National Bureau of Standards.

Davy, N. 1944 *Phil. Mag.* **35** (7), 819–840.

Dean, W. R. 1945 *Proc. Camb. Phil. Soc.* **41**, 231–238.

Flagg, C. N. & Newman, J. N. 1971 *J. Ship Res.* **15**, 257–265.

Guiney, D. C. 1972 Ph.D. thesis, University of Adelaide.

Lewin, M. 1963 *J. Math. Phys.* **42**, 287–300.

Mei, C. C. 1966 *Quart. J. Mech. Appl. Math.* **19**, 417–440.

Newman, J. N. 1969 *J. Fluid Mech.* **39**, 97–115.

Ogilvie, T. F. 1960 Ph.D. thesis, University of California, Berkeley.

Porter, D. 1972 *Proc. Camb. Phil. Soc.* **71**, 411–421.

Taylor, P. J. 1971 Ph.D. thesis, University of Adelaide.

Tuck, E. O. 1971 *J. Fluid Mech.* **49**, 65–73.

Tuck, E. O. & Taylor, P. J. 1970 *8th Symp. Nav. Hydro.*, Office of Naval Research, Washington D.C.

Ursell, F. 1947 *Proc. Camb. Phil. Soc.* **43**, 374–382.

Wehausen, J. V. & Laitone, E. V. 1960 *Handbook of Physics*, vol. 9. *Surface Waves.* Springer.